Study on the Extent of Folding Back Conformation in Poly(aryl ether) Dendrimers by Intramolecular Electron Transfer and Exciplex Formation

Ying-Ying Li,[†,‡] Lei Han,[†,‡] Jinping Chen,[†] Shaojun Zheng,[†,‡] Yi Zen,[†,‡] and Yi Li*[,†]

Laboratory of Organic Optoelectronic Functional Materials and Molecular Engineering, Technical Institute of Physics and Chemistry, Chinese Academy of Sciences, Beijing 100080, P. R. China, and Graduate School, Chinese Academy of Sciences, Beijing 100039, P. R. China

Shayu Li[§] and Guoqiang Yang*[,§]

Beijing National Laboratory for Molecular Sciences (BNLMS), Key Laboratory of Photochemistry, Institute of Chemistry, Chinese Academy of Sciences, Beijing 100080, P. R. China

Received August 22, 2007; Revised Manuscript Received October 23, 2007

ABSTRACT: A series of poly(aryl ether) dendrimers (Py−G*n*−NHPh, $n = 1-4$) with only one pyrene chromophore at the periphery and an aniline group at the core were synthesized and the extent of folding back conformation was given by the intramolecular electron transfer and exciplex formation. Selective excitation of the periphery pyrene moiety of Py−G*n*−NHPh in dichloromethane resulted in an electron-transfer process from aniline to pyrene, and as a consequence of the electron transfer, an intramolecular exciplex was formed. Since the exciplex formation requires a direct orbital overlap between the donor and the acceptor groups, this gives us a direct experimental observation for the folding back conformation of poly(aryl ether) dendrimers. The efficiencies and the rate constants of electron transfer in dichloromethane are measured to be 0.90, 0.83, 0.78, 0.68, and 3.6×10^8, 1.7×10^8, 1.2×10^8, and 6.6×10^7 s^{-1} for generations 1−4, respectively. The separations (center to center) between the core donor group and the periphery acceptor chromophore are estimated from the rate constants of electron transfer, which are 7.7, 8.0, 8.2, and 8.5 Å for generations 1−4, respectively. This means that the periphery chromophores can fold inward and reach to the core vicinity for all four generations.

Introduction

Dendrimers are regularly and hierarchically branched macromolecules with numerous chain ends all emanating from a single core.[1] The chromophores can be accurately located at the core, focal point, periphery, or even at each branching point of the dendritic structure. Manipulation of dendrimer size, shape, and properties promises to provide a wide range of materials with different potential applications,[2] including catalysis,[3] self-assembly,[4] molecular recognition, and encapsulation.[5]

The chemical structure of dendrimers can be characterized spectroscopically; however, the detailed three-dimensional structures of dendrimers are still not well-understood. A thorough understanding of the molecular structure, including microstructure and conformation, will promote applications of dendrimers. In the early 1980s, de Gennes and Hervet proposed a molecular structure with a dense shell and a loose core;[6] while later, Lescanec and Muthukumar predicted a density maximum in the center of dendrimers in 1990.[7] Since then, numerous theoretical and experimental studies have been conducted to verify their findings. Computational investigations through molecular dynamics[8,9] and Monte Carlo[10,11] simulations indicate that a significant backfolding of the end groups into the interior occurs in flexible dendritic structures, which is more or less in line with the Lescanec−Muthukumar model, while the experiment results confirmed this theoretical prediction. Many experimental studies on different dendrimers have been reported using, e.g., size-exclusion chromatography (SEC), viscosimetry,[9,12] NMR studies,[13,14] solvatochromic probe,[15] and fluorescence depolarization.[16] There are several studies on poly(aryl ether) dendrimers to establish the possibility of backfolding in these molecules. Mourey et al.,[12] using size exclusion chromatography coupled with molecular weight sensitive detection, suggest that the density of these dendrimers decreases monotonically from the center, which is in agreement with the model proposed by Lescanec and Muthukumar. Hawker et al.[15] attached a solvatochromism chromophore, 4-(*N*,*N*-dimethyl)-1-nitrobenzene, to the focal point of various generations of poly(aryl ether) dendrimers. Studies on the change of the absorption maximum for the solvatochromism core group in different solvents indicate that there is a transition in the shape of dendrimers from an extended structure to a globular one from generation three to generation four. Rotational-echo double-resonance (REDOR) NMR studies on Fréchet-type dendrimers by Wooley et al. illustrate that the backfolding can also take place in the solid state.[13] In addition, Gorman et al.[14] measured the spin lattice relaxation (T_1, longitudinal relaxation time constants) in poly(aryl ether) dendrimers with a paramagnetic core. The data reveal that the end groups are close to the core in space. De Schryver and co-workers[16] provided an example of the hydrodynamic volume studies for Fréchet-type dendrimers with a rubicene core by fluorescence depolarization measurements and concluded that the dendrimer became more and more dense with the generation increase and the quality decrease of solvents. Recently, our studies[17] show that the intramolecular triplet energy transfer and electron transfer from the periphery

* To whom correspondence should be addressed.
† Technical Institute of Physics and Chemistry, Chinese Academy of Sciences.
‡ Graduate School, Chinese Academy of Sciences.
§ Institute of Chemistry, Chinese Academy of Sciences.

10.1021/ma071901w CCC: $37.00
Published on Web 12/04/2007

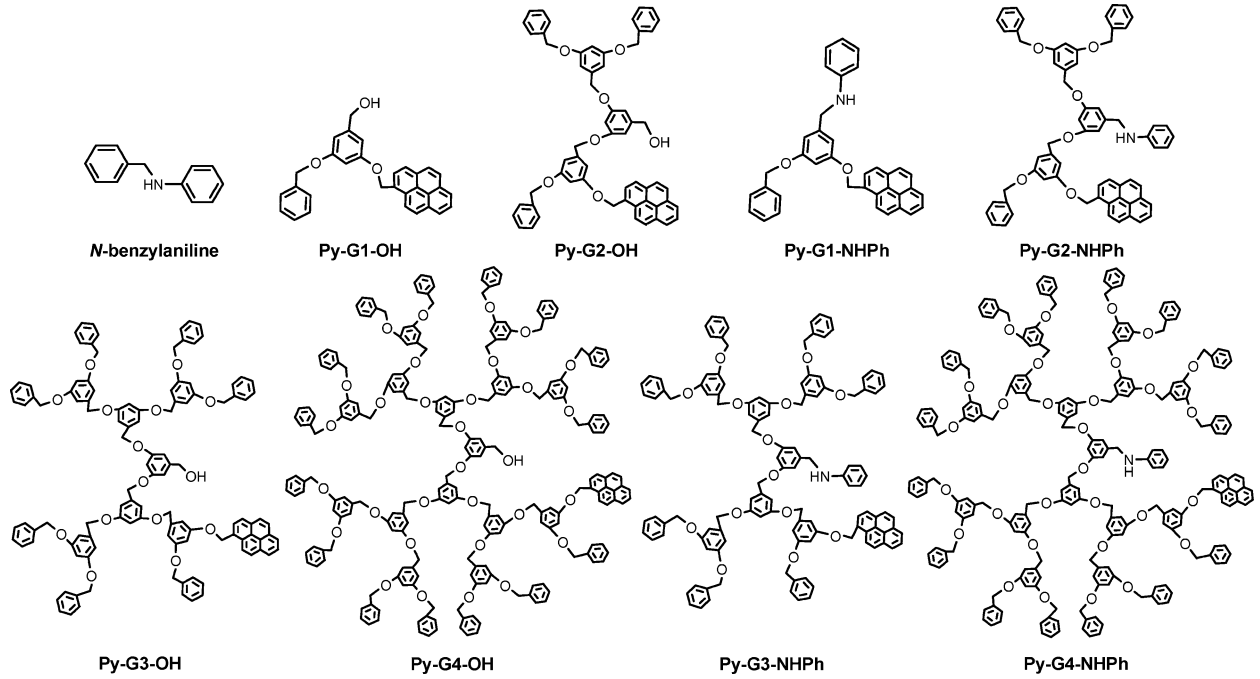

Figure 1. Structures of *N*-benzylaniline, Py−G*n*−OH and Py−G*n*−NHPh.

Scheme 1. Synthesis of Py−G*n*−OH and Py−G*n*−NHPh[a]

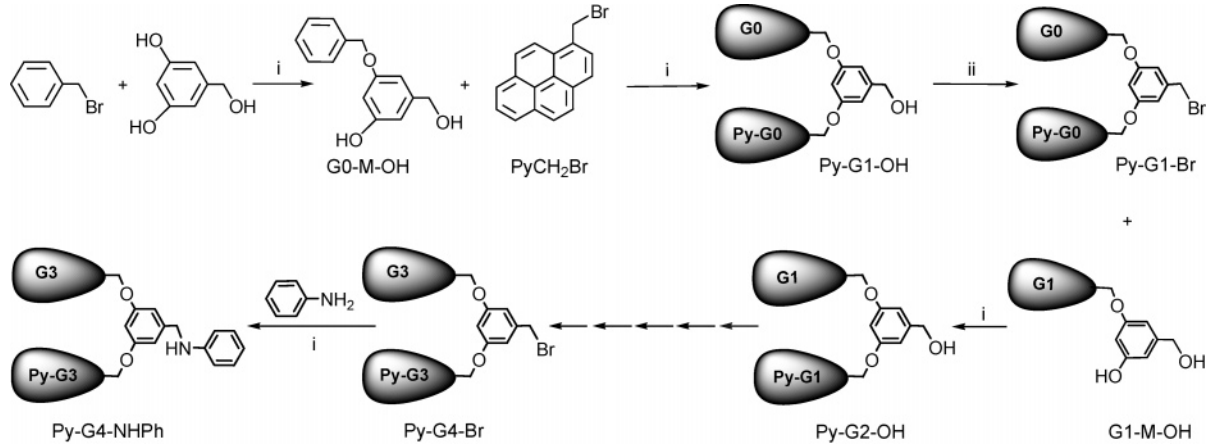

[a] Reagents: i, K_2CO_3, 18-C-6; ii, CBr_4, PPh_3.

groups to the core in poly(aryl ether) dendrimers can occur efficiently. We proposed that the triplet energy transfer and electron-transfer proceed mainly via a through-space mechanism involving the closest donor (folding back conformation) and acceptor groups.

Many research results suggest that poly(aryl ether) dendrimers take a folding back conformation. However, there is still a lack of direct experimental evidence to give a quantitative description on the folding back conformation for poly(aryl ether) dendrimers. In this contribution, we create a dendritic system (Py−G*n*−NHPh) in which one pyrene chromophore and one aniline group are attached to the periphery and the core of poly(aryl ether) dendrimers, respectively. The formation of an exciplex between the intramolecular periphery pyrene and the core aniline groups is used as the probe to detect the folding back occurrence of the dendrimer backbone, and the extent of the periphery group folded into the core is then analyzed using an intramolecular photoinduced electron-transfer based fluorescence quenching process between the pyrene and the aniline groups. The dendrimers are synthesized up to the fourth generation, as shown in Figure 1.

Results and Discussion

Synthesis of the Dendrimers. A typical donor−acceptor pair (*N*,*N*-dimethylaniline−pyrene),[18] in which an exciplex will form through the photoinduced electron transfer, is chosen to be attached to the core and the periphery, respectively. To avoid the interference of the excimer formation between periphery pyrene chromophores on the observation of the exciplex formation, only one end group is substituted by the pyrene chromophore in Py−G*n*−NHPh. It should be pointed out that all the periphery positions are equivalent. One pyrene group functionalized dendritic benzyl alcohols (Py−G*n*−OH) and dendritic benzyl bromides (Py−G*n*−Br) were synthesized by Fréchet's method.[19] The schematic synthesis route is shown in Scheme 1. By using a much more excessive amount of the monomer unit, 3,5-dihydroxybenzyl alcohol, we monoalkylate the 3,5-dihydroxybenzyl alcohol with benzyl bromide to give a monophenol G0−M−OH. Alkylation of the monophenol G0−M−OH with 1 mol equiv of 1-bromomethylpyrene introduced a functional group to the periphery of the dendrimer and gave the first generation, unsymmetrical benzyl alcohol Py−G1−OH. Repeating the monoalkylation of the 3,5-dihydroxybenzyl

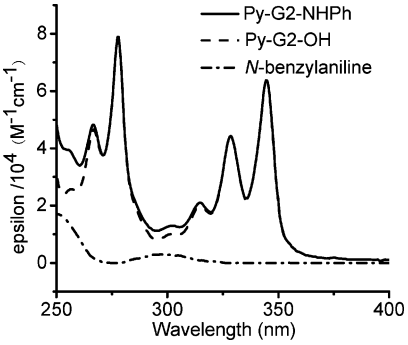

Figure 2. Absorption spectra for the donor model compound *N*-benzylaniline, the acceptor model compound Py−G2−OH, and the target compound Py−G2−NHPh in CH_2Cl_2.

alcohol and the alkylation of the monophenol by using nonfunctional dendron and monofunctional dendron, respectively, gave one pyrene group functionalized dendron Py−G*n*−OH. The target compounds Py−G*n*−NHPh were synthesized with dendritic benzyl bromides (Py−G*n*−Br) and aniline. The details of the synthesis and purification of Py−G*n*−OH and Py−G*n*−NHPh ($n = 1-4$) are described in the Experimental Section. The target compounds Py−G*n*−NHPh ($n = 1-4$) and the model compounds Py−G*n*−OH were characterized by ^{1}H NMR, ^{13}C NMR, IR, mass spectrometry (MALDI-TOF), and HPLC.

Exciplex Formation as a Probe to Detect the Backfolding Conformation of Poly(aryl ether) Dendrimers. First the absorption spectra of the target compounds (Py−G*n*−NHPh) and their model compounds (Py−G*n*−OH and *N*-benzylaniline, structures are also shown in Figure 1) were measured in dichloromethane (CH_2Cl_2). Figure 2 illustrates the absorption spectra of Py−G2−NHPh and Py−G2−OH, combined with that of the donor model compound *N*-benzylaniline. The absorption bands characteristics of the poly(aryl ether) dendron and the pyrene chromophore dominate the whole spectra of Py−G*n*−NHPh and Py−G*n*−OH. The ground state behavior of Py−G*n*−NHPh can be studied in comparison with the corresponding model compound Py−G*n*−OH and *N*-benzylaniline. The absorption spectrum of Py−G*n*−NHPh closely matches the sum of absorptions of the donor and the acceptor model compounds. This means that there is no measurable interaction between the pyrene and the *N*-benzylaniline chromophores in Py−G*n*−NHPh. Significantly, there is only pyrene chromophore absorption bands above 325 nm. Thus, the singlet−singlet energy transfer from the excited pyrene chromophore to the aniline group is impossible. Furthermore, this fact permits the selective excitation of the pyrene moiety in Py−G*n*−NHPh.

The fluorescence spectra of Py−G*n*−NHPh and a comparison one of Py−G4−NHPh and Py−G4−OH in CH_2Cl_2 are presented in Figure 3. The fluorescence characteristic of pyrene with maxima at 378 and 396 nm and a shoulder at 386 nm was detected for both Py−G*n*−NHPh and Py−G*n*−OH with selective excitation of pyrene. In addition, Py−G*n*−NHPh shows a structureless band appearing at longer wavelength, which is assigned to the exciplex emission between the periphery pyrene chromophore and the core aniline group,[18] and measurements at different concentrations reveal that the exciplex formation is intramolecular. With the exception of the fluorescence shape difference, the fluorescence efficiency of the pyrene chromophore in Py−G*n*−NHPh is lower than that of the corresponding model compound Py−G*n*−OH for G1−G4. This finding indicates that the fluorescence of pyrene is quenched by the core aniline group in Py−G*n*−NHPh dendrimers. The independency of concentrations manifests that the quenching is intramolecular. The intramolecular fluorescence quenching data are given in Table 1.

Since the possibility of singlet−singlet energy transfer being responsible for the intramolecular pyrene fluorescence quenching by the aniline group in Py−G*n*−NHPh is excluded on thermodynamic grounds, as mentioned above, we analyzed the reality of electron transfer between the pyrene chromophore and the aniline group as the cause of the fluorescence quenching. The free energy change (ΔG in kcal/mol) involved in an electron-transfer process can be estimated by eq 1:[20]

$$\Delta G = 23.06[E(D^{\bullet+}/D) - E(A/A^{\bullet-})] - E_{00} - (e^2/r\epsilon) - (e^2/2)((1/r_+) + (1/r_-))((1/37.0) - (1/\epsilon)) \quad (1)$$

E_{00} represents the singlet excited-state energy of the pyrene group (77.0 kcal/mol)[21a] here. $E(D^{\bullet+}/D)$ and $E(A/A^{\bullet-})$ are +0.81 and −1.79 eV in acetonitrile.[21] The distance between the donor and the acceptor (r) is about 7.7, 8.0, 8.2, and 8.5 Å for generations 1−4, respectively (see estimation in section of the study of the extent of folding back conformation). The last term in eq 1 is the Born correction to the solvation energy which depends on the radius of the donor cation (r_+) and the acceptor anion (r_-). To estimate the Born correction to the solvation energy, we set r_+ and r_- equal to 3 and 4 Å, respectively, by assuming that both donor and acceptor are spherical. Estimation from eq 1 shows that the electron transfer from the aniline group to the singlet excited pyrene portion of Py−G*n*−NHPh in CH_2Cl_2 ($\epsilon = 9.14$)[22] is exothermic by 13.7∼13.3 kcal/mol for generations 1−4. Therefore, the fluorescence quenching of the pyrene chromophore in Py−G*n*−NHPh is caused by the intramolecular electron transfer between the pyrene and the aniline groups. As a consequence of the electron-transfer process, an exciplex is formed.

The exciplex formation requires a direct orbital overlap between the donor and the acceptor; it has been suggested that the optimal distance of the D−A pair is between 3 and 7 Å.[23] The distance between the periphery chromophore and the core group in Py−G*n*−NHPh bearing a full stretched conformation can be estimated by using the HyperChem 6.0 program, which is 10, 17, 24, and 31 Å for generation 1−4, respectively; within these distances the exciplex could not exist likely and this is quite contrary to the experimental results. As a matter of fact, the intramolecular exciplex formation is observed for Py−G*n*−NHPh ($n = 1-4$) in CH_2Cl_2, which means that dendrimers must take a folded conformation making the periphery pyrene chromophore and the core aniline group close to each other. This gives us a direct experimental observation for the folding back conformation of poly(aryl ether) dendrimers.

Study on the Extent of Folding Back Conformation in Py−G*n*−NHPh by Time-Resolved Spectroscopy. The fluorescence lifetimes for Py−G*n*−NHPh and Py−G*n*−OH were determined in dichloromethane at ambient conditions. The excitation wavelength was 345 nm, and the fluorescence decay was monitored at 378 (the pyrene emission maximum) and 498 nm (the exciplex emission maximum) for Py−G*n*−NHPh and 378 nm only for Py−G*n*−OH, respectively. All the compounds we investigated exhibit monoexponential profiles at 378 nm, but the decay curves obtained at 498 nm cannot be fitted well to give quality lifetime data due to the weak exciplex emission. All the lifetime data are summarized in Table 2. Figure 4 shows

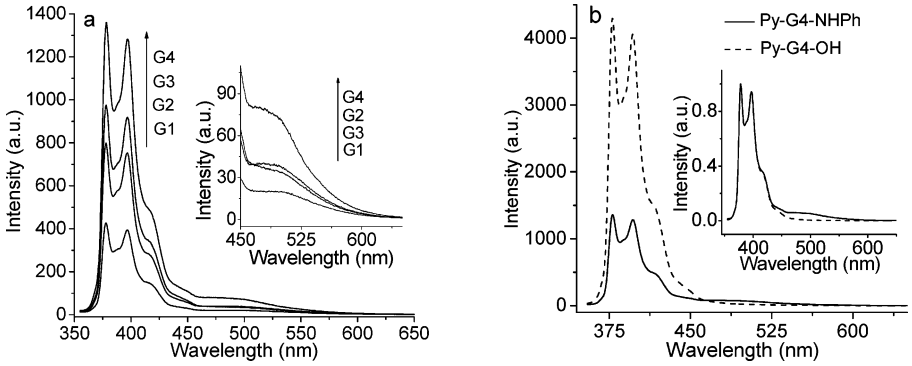

Figure 3. Fluorescence spectra of Py−G*n*−NHPh ($n = 1-4$) (a) and a comparison one of Py−G4−NHPh and Py−G4−OH in CH_2Cl_2 (b). λ_{ex} = 345 nm, [Py−G*n*−NHPh] = [Py−G4−OH] = 1.5×10^{-6} M.

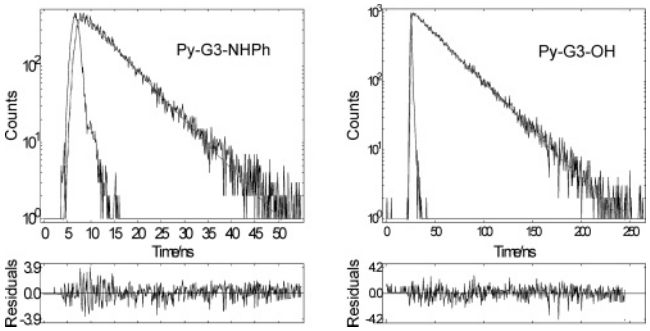

Figure 4. Fluorescence decay traces of Py−G3−NHPh and Py−G3−OH in CH_2Cl_2 at ambient with the excitation λ_{ex} = 345 nm and the detection λ = 378 nm. [Py−G3−NHPh] = [Py−G3−OH] = 2×10^{-6} M. The sharp decay curve is the lamp profile, and the blue solid line is the fitted curve. The bottom trace shows the residuals distribution for the monoexponential fit.

Table 1. Electron-Transfer Efficiencies, Rate Constants, and Estimated Donor−Acceptor Distance for Compounds Py−G*n*−NHPh

	Φ_{ET}[a]	Φ_{ET}[b]	k_{ET} (s^{-1})	r[c] (Å)
G1	0.87	0.90	3.6×10^8	7.7
G2	0.78	0.83	1.7×10^8	8.0
G3	0.74	0.78	1.2×10^8	8.2
G4	0.68	0.68	6.6×10^7	8.5

[a] Determined by steady-state fluorescence measurements. [b] Determined by time-resolved fluorescence spectroscopy. [c] Estimated from eq 4.

Table 2. Fluorescence Lifetime for Dendrimers Py−G*n*−NHPh and Py−G*n*−OH in CH_2Cl_2

	target compound		model compound	
compound	τ (ns)	χ^2	τ (ns)	χ^2
G1	2.6	1.103	27.4	0.978
G2	4.8	1.040	28.1	0.968
G3	6.7	1.050	30.6	0.999
G4	10.4	1.176	32.6	1.048

the decay curves of Py−G3−NHPh and Py−G3−OH at 378 nm in CH_2Cl_2. The rate constants (k_{ET}) and the efficiencies (Φ_{ET}) of electron transfer can be calculated from the lifetimes of Py−G*n*−NHPh (τ_{NHP}) and Py−G*n*−OH (τ_{OH}) according to eqs 2 and 3, respectively, and the results are shown in Table 1. The electron-transfer efficiencies are 0.90, 0.83, 0.78, and 0.68 for generations 1−4, respectively, which are comparable with those obtained from the fluorescence efficiency measurements. The rate constants are 3.6×10^8, 1.7×10^8, 1.2×10^8, and 6.6×10^7 s^{-1} for generations 1−4, respectively, which only decreases slightly as the generation increases. This is similar to what we observed before.[17b]

$$k_{ET} = (1/\tau_{NHP}) - (1/\tau_{OH}) \quad (2)$$

$$\Phi_{ET} = 1 - (\tau_{NHP}/\tau_{OH}) \quad (3)$$

It has been established that the electron transfer requires a strong donor−acceptor orbital overlap, and the rate constant will decrease exponentially with increasing donor−acceptor distance. Thus, one might expect that the rate constant of electron transfer will become negligibly small as the donor−acceptor distance increases beyond the sum of their van der Waals radii (5−10 Å) except it occurs via a "through-bond mechanism". Since the Py−G*n*−NHPh dendrimer is not a conjugated or a rigid system and the rate constant of the intramolecular electron transfer in Py−G*n*−NHPh does not decrease exponentially with increasing generation, the "through-bond mechanism" can be excluded in our study. Therefore, we infer that the intramolecular electron transfer between the pyrene and the aniline groups in Py−G*n*−NHPh mainly proceeds via a "through-space mechanism". Estimation with HyperChem 6.0 gives the van der Waals radii of the donor aniline group and the acceptor pyrene chromophore to be 3.3 and 3.7 Å, respectively, by assuming that both donor and acceptor are spherical. If the Py−G*n*−NHPh molecules took a stretched conformation, the intramolecular electron-transfer would not occur efficiently, because the separation of the donor and the acceptor (it is 10, 17, 24, and 31 Å for generations 1−4, respectively) would be much larger than the sum of the van der Waals radii of aniline and pyrene (7 Å). This is contrary to the experimental results. Obviously, Py−G*n*−NHPh must take a folded conformation to shorten the distance of the periphery pyrene and the core aniline groups, and then the intramolecular electron transfer occurs between the approaching donor and acceptor groups via a through-space mechanism.

How much is the extent of the Py−G*n*−NHPh molecules folding back? We use the intramolecular electron-transfer rate constant to estimate the separation of donor and acceptor, which is utilized as a measure of the extent of folded conformation. In terms of most quantum mechanical descriptions, electron transfer is the "super-molecule" approach in which the electron donor, acceptor, and solvent are treated as a single system. Within this framework, first-order perturbation theory treatments of nonadiabatic electron-transfer reactions occurring via tunneling have been presented by many groups.[24] According to these quantum mechanical descriptions and a common approximation,[24c,25] the electron-transfer rate constant ($k(r)$ in

units of s^{-1}) for one vibrational level of the reactants at fixed donor−acceptor distance, r, can be given by eq 4:

$$k(r) = \upsilon_0 F \exp[-2(r - r_0)/\alpha] \quad (4)$$

where F is the thermally averaged Franck−Condon factor, the frequency factor υ_0 is proportional to a Franck−Condon weighted density of states, which depends on the exothermicity, $-\Delta G^0_{ET}$, of the electron-transfer reaction, r is the distance between donor and acceptor, r_0 is a small correction for the finite radii of donor and acceptor, and the range parameter α determines the steepness of the rate−distance dependence.[26] According to the literature, the typical υ_0 is 10^{15} s^{-1}, α is typically near 1 Å, and we set r_0 equal to 6 Å in Py−G*n*−NHPh. The reaction exothermicity of electron transfer in Py−G*n*−NHPh dendrimers is about 0.55 eV (CH_2Cl_2); thus, the corresponding Franck−Condon factor (F) in this system is estimated to be 10^{-5} from the relationship between the relative electron-transfer rate and the reaction exothermicity.[26] Assuming the conformation of the investigated molecules Py−G*n*−NHPh to be frozen at the moment of electron transfer occurrence, the distance (r) between the donor *N*-methyl aniline and the acceptor pyrene for each molecule is fixed. The calculated electron-transfer rate constants from the fluorescence lifetime data, 3.6×10^8, 1.7×10^8, 1.2×10^8, and 6.6×10^7 s^{-1} for generations 1−4, respectively, represent the average one for all molecules in the system. With all these considerations, the average distance between donor and acceptor (r) in Py−G*n*−NHPh dendrimers can be estimated to be 7.7, 8.0, 8.2, and 8.5 Å for generations 1−4, respectively, by using eq 4. The result is in agreement with recent research results.[13,17,27]

Each generation increase of poly(aryl ether) dendrimers means adding one layer of the benzyloxy unit, whose size is about 6.3 Å. The estimation result shows that the average donor−acceptor distance in Py−G*n*−NHPh only increases 0.8 Å from G1 to G4. Enlarging the molecular size by three layers with only less than 1 Å increase of the separation between the periphery acceptor and the core donor indicates that the Py−G*n*−NHPh molecules are extremely folded. Considering that the sum of the van der Waals radii of donor and acceptor is about 7 Å, the estimated value r (7.7, 8.0, 8.2, and 8.5 Å for generations 1−4, respectively) demonstrates that the periphery chromophores can fold inward and reach to the core vicinity for all four generations. The extent of the folding back conformation for poly(aryl ether) dendrimers is given quantifiably by experimental results. The visual expression of the folded Py−G*n*−NHPh molecules is shown in Figure 5. The distinct gray global shape represents the dendrimer molecule corresponding to each generation with different size. The aniline group (blue) is assumed to be located at the core area, while the different location of the pyrene chromophores (red) indicates the relative distance between the periphery acceptor and the core donor with varied generation.

We also tried to get the information of electron transfer in Py−G*n*−NHPh by the transient absorption measurements. Pulsed-laser photolysis of the mixture of pyrene and *N*-benzylaniline was performed in deuterated solvent (CH_3CN−THF = 3:1) by using 355 nm excitation light, which gives rise to a strong transient absorption with maxima at 415 and 495 nm (Figure 6). The absorption at 415 and 495 nm are assigned to the triplet state and the radical anion of the pyrene chromophore, respectively, by reference to the transient absorption of pyrene.[28] Pulsed laser photolysis of Py−G*n*−NHPh under identical conditions only leads to a strong transient absorption of the triplet state of the pyrene chromophore with a maximum at 415 nm (Figure 6). No transient absorption assigned to the radical anion of pyrene is observed in Py−G*n*−NHPh (n = 1−4). This might be explained by the destabilization of the pyrene radical anion in Py−G*n*−NHPh. When the lifetime of transient absorption species is shorter than the equipment response time (10 ns), no signal can likely be detected. Like most published work,[29] the transient absorption of the aniline cation can be detected neither in the mixture of pyrene and *N*-benzylaniline nor in Py−G*n*−NHPh because of its very small transient absorption coefficient.

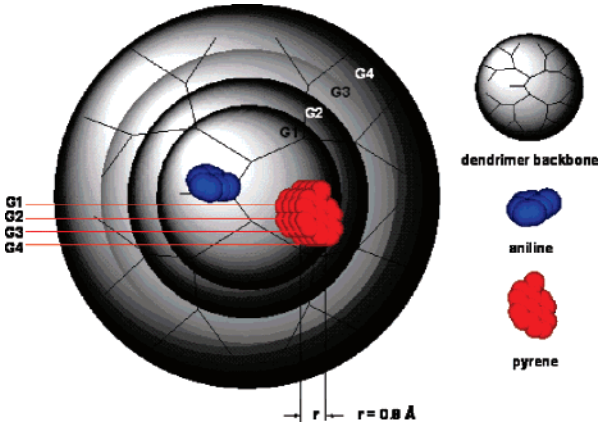

Figure 5. The visual expression of the relative distance of donor and acceptor with the molecular size increase of Py−G*n*−NHPh.

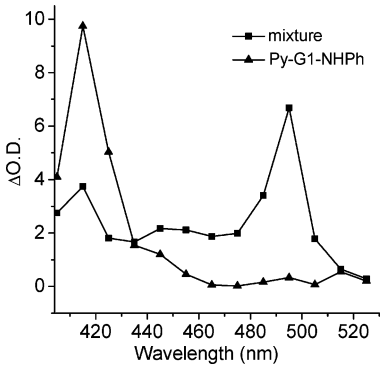

Figure 6. Transient absorption spectra of the mixture of pyrene and *N*-benzylaniline and Py−G1−NHPh in the solvent, CH_3CN−THF = 3:1, at the peak of the laser pause. (λ_{ex} = 355 nm, [pyrene] = [Py−G1−NHPh] = 2×10^{-4} M, [*N*-benzylaniline] = 2×10^{-1} M).

Conclusions

Understanding of the dendrimer conformation is very important for expanding the applications of dendritic systems. Our approach of the development of the pyrene−aniline functionalized dendrimer Py−G*n*−NHPh has allowed us to know some details of the poly(aryl ether) dendrimer conformation. The steady state and time-resolved fluorescence spectroscopy studies reveal that Py−G*n*−NHPh undergoes the singlet electron-transfer process in dichloromethane. The efficiencies and the rate constants of electron transfer in CH_2Cl_2 are 0.90, 0.83, 0.78, 0.68 and 3.6×10^8, 1.7×10^8, 1.2×10^8, 6.6×10^7 s^{-1} for generations 1−4, respectively. As a consequence of the electron-transfer process, an intramolecular exciplex between the periphery pyrene chromophore and the core aniline group is formed, which gives a direct experimental observation of the folding back conformation of poly(aryl ether) dendrimers. Moreover, estimation from the rate constants of electron-transfer based on the "super-molecule" descriptions results in a particular value of the distance between donor and acceptor, 7.7, 8.0, 8.2,

and 8.5 Å, for generations 1−4, respectively. This means that the periphery chromophores can fold inward and reach to the core vicinity for all four generations. To a certain extent, our results are somewhat consistent with the model proposed by Lescanec and Muthukumar. These findings provide a substantial insight into the folding back conformation of poly(aryl ether) dendrimers.

Experimental Section

Materials. Reagents were purchased from Aldrich or Acros and were used without further purification, unless otherwise noted. Tetrahydrofuran was distilled over Na/benzophenone under an argon atmosphere. Acetone was dried with anhydrous K_2CO_3 and distilled. Spectral-grade CH_2Cl_2 was used for steady-state and time-resolved spectroscopy measurements.

Instrumentation. ^{1}H NMR and ^{13}C NMR spectra were recorded on either a Varian Gemini 300 MHz or a Bruker 400 MHz spectrometer. IR spectra were run on a Bio-Rad Win IR spectrometer. MALDI-TOF mass spectrometry was performed on a Bruker BIFLEX spectrometer. HPLC was recorded on a Hitachi system with a Diamonsil C18 5 μm column (4.6 mm i.d., 25 cm) and a UV−vis detector. Steady-state absorption spectra and fluorescence spectra were measured by a Shimadzu UV-1601PC spectrometer and a Hitachi F-4500 spectrometer, respectively.

Fluorescence Measurements. Fluorescence spectra were measured in CH_2Cl_2 using a 1 cm quartz cuvette at room temperature (RT). The excitation wavelength was 345 nm. To compare the emission efficiency of Py−G*n*−NHPh and Py−G*n*−OH, solutions at the excitation wavelength have the same optical density. The relative emission efficiencies were obtained from the peak areas of emission spectra.

Time-Resolved Spectroscopic Measurements. Fluorescence decay processes were recorded with a single photon counting technique on an Edinburgh FLS920 fluorescence lifetime system, and the equipment resolution is ∼0.1 ns. Nanosecond transient absorption spectra were performed on a LP-920 pump−probe spectroscopic setup (Edinburgh). The excited light source was an unfocused third harmonic (355 nm, 7 ns fwhm) output of a Nd:YAG laser (Continuum surelite II), and the probe light source was a pulse-xenon lamp. The signals were detected by an Edinburgh analytical instrument (LP900) and recorded on a Tektronix TDS 3012B oscilloscope and computer.

General Procedure for the Synthesis of Py−G*n*−OH. A mixture of the appropriate monopyrene-substituted bromide (1.00 mol equiv), the corresponding monophenolic derivative (1.00 mol equiv), potassium carbonate (2.00 mol equiv), and 18-crown-6 (0.2 mol equiv) in dry acetone was heated at reflux under nitrogen for 48 h. The mixture was cooled, evaporated to dryness, and partitioned between CH_2Cl_2 and water. The aqueous layer was extracted with CH_2Cl_2 (3×), and the combined organic layers were dried and evaporated to dryness. The crude product was purified as outlined in the following text.

Py−G1−OH. It was prepared from 3-benzyloxy-5-hydroxybenzyl alcohol (G0−M−OH) and 1-bromomethylpyrene, purified by column chromatography on silica gel (CH_2Cl_2−Et_2O = 50:1) to give Py−G1−OH as a white solid. Yield 70%; retention time t_R = 10.2 min in HPLC (acetonitrile−THF = 10:1), purity 98%; IR ν 3560, 3062, 3034, 2923, 2872, 1598, 1454, 1374, 1162, 1065 cm^{-1}; ^{1}H NMR ($CDCl_3$) δ 4.68 (d, 2H, J = 6 Hz, −CH_2OH), 5.06 (s, 2H, −OCH_2Ar), 5.75 (s, 2H, −OCH_2Py), 6.69 (s, 2H, ArH), 6.77 (s, 1H, ArH), 7.30−7.41 (m, 5H, ArH), 8.04−8.31 (m, 9H, PyH); MS (MALDI-TOF) *m*/*z* 443.5 (M − 1), 467.4 (M + Na^+), 483.4 (M + K^+), calcd *m*/*z* 444.17.

Py−G2−OH. It was prepared from G1−M−OH and Py−G1−Br, purified by column chromatography eluting with dichloromethane to give Py−G2−OH as a colorless glassy solid. Yield 75%; retention time t_R = 13.3 min in HPLC (acetonitrile−THF = 10:1), purity 97%; IR ν 3561, 3062, 3037, 2923, 2865, 1596, 1497, 1450, 1378, 1160, 1061 cm^{-1}; ^{1}H NMR ($CDCl_3$) δ 4.61 (d, 2H, J = 6 Hz, −CH_2OH), 4.98−5.05 (m, 10H, −OCH_2Ar), 5.74 (s, 2H, −OCH_2Py), 6.54−6.83 (m, 9H, ArH), 7.31−7.42 (m, 15H, ArH), 8.03−8.31 (m, 9H, PyH); MS (MALDI-TOF) *m*/*z* 867.7 (M − 1), 891.7 (M + Na^+), 907.7 (M + K^+), calcd *m*/*z* 868.34.

Py−G3−OH. It was prepared from G2−M−OH and Py−G2−Br, purified by column chromatography on silica gel (CH_2Cl_2−Et_2O = 50:1) to give Py−G3−OH as a colorless glassy solid. Yield 80%; retention time t_R = 23.9 min in HPLC (acetonitrile−THF = 10:1), purity 99%; IR ν 3562, 3089, 3062, 3031, 2930, 2873, 1595, 1448, 1372, 1156, 1046 cm^{-1}; ^{1}H NMR ($CDCl_3$) δ 4.56 (s, 2H, −CH_2OH), 4.94−5.02 (m, 26H, −OCH_2Ar), 5.70 (s, 2H, −OCH_2Py), 6.53−6.81 (m, 21H, ArH), 7.30−7.39 (m, 35H, ArH), 7.98−8.29 (m, 9H, PyH); MS (MALDI-TOF) *m*/*z* 1740.0 (M + Na^+), 1756.0 (M + K^+), calcd *m*/*z* 1716.67.

Py−G4−OH. It was prepared from G3−M−OH and Py−G3−Br, purified by column chromatography on silica gel (CH_2Cl_2−Et_2O = 100:1) to give Py−G4−OH as a colorless glassy solid. Yield 72%; retention time t_R = 18.4 min in HPLC (acetonitrile−THF = 4:1), purity 99%; IR ν 3538, 3088, 3062, 3030, 2926, 2870, 1594, 1448, 1371, 1150, 1044 cm^{-1}; ^{1}H NMR ($CDCl_3$) δ 4.48 (s, 2H, −CH_2OH), 4.89−4.97 (m, 58H, −OCH_2Ar), 5.65 (s, 2H, −OCH_2Py), 6.32−6.67 (m, 45H, ArH), 7.28−7.36 (m, 75H, ArH), 7.96−8.21 (m, 9H, PyH); MS (MALDI-TOF) *m*/*z* 3436.8 (M + Na^+), 3452.8 (M + K^+), calcd *m*/*z* 3413.34.

General Procedure for the Synthesis of Py−G*n*−NHPh. The reactions were carried out on scales of about 200 mg. A mixture of the appropriate dendritic benzyl bromide, Py−G*n*−Br (1.00 mol equiv), aniline (5.00 mol equiv), potassium carbonate (7.5 mol equiv), and 18-crown-6 (0.6 mol equiv) in dry acetone was stirred under nitrogen for 24 h. The mixture was then cooled and evaporated to dryness. The residue was partitioned between water and CH_2Cl_2; the water layer was then extracted with CH_2Cl_2 (3 × 20 mL), and the combined organic layers were dried over $MgSO_4$ and evaporated to dryness. The crude product was purified as outlined in the following text.

Py−G1−NHPh. It was prepared from Py−G1−Br and aniline, purified by column chromatography eluting with petroleum ether−dichloromethane (1:3) to give Py−G1−NHPh as a pale-yellow solid. Yield 85%; retention time t_R = 11.1 min in HPLC (acetonitrile−THF = 6.5:1), purity 98%; IR ν 3419, 3084, 3062, 3032, 2925, 2870, 1602, 1453, 1365, 1329, 1154, 1065 cm^{-1}; ^{1}H NMR ($CDCl_3$) δ 4.30 (s, 2H, −CH_2N−), 5.03 (s, 2H, −OCH_2Ar), 5.72 (s, 2H, −OCH_2Py), 6.63−6.78 (m, 5H, ArH), 7.15−7.19 (m, 2H, ArH), 7.31−7.41 (m, 6H, ArH), 8.01−8.31 (m, 9H, PyH); ^{13}C NMR ($CDCl_3$) δ 48.6 (−CH_2NH−), 69.0 (−OCH_2Py), 70.2 (−OCH_2Ar), 101.2, 106.7, 106.8, 113.0, 117.8, 123.2, 124.8, 125.1, 125.5, 126.2, 127.0, 127.5, 127.7, 127.8, 128.1, 128.2, 128.7, 129.4, 129.8, 130.9, 131.4, 131.7, 137.0 (Py C), 142.4 (Ar C), 148.2 (−NHPh C), 160.4, 160.5 (−OPh C); MS (MALDI-TOF) *m*/*z* 518.3 (M − 1), 542.3 (M + Na^+), 558.3 (M + K^+), calcd *m*/*z* 519.22.

Py−G2−NHPh. It was prepared from Py−G2−Br and aniline, purified by column chromatography on silica gel (CH_2Cl_2−Et_2O = 400:1) to give Py−G2−NHPh as a pale-yellow glassy solid. Yield 82%; retention time t_R = 13.4 min in HPLC (acetonitrile−THF = 6.5:1), purity 98%; IR ν 3420, 3085, 3062, 3030, 2933, 2879, 2860, 1595, 1498, 1453, 1370, 1160, 1055 cm^{-1}; ^{1}H NMR ($CDCl_3$) δ 4.31 (s, 2H, −CH_2N−), 5.01−5.12 (m, 10H, −OCH_2Ar), 5.80 (s, 2H, −OCH_2Py), 6.57−6.89 (m, 14H, ArH), 7.21−7.25 (m, 2H, ArH), 7.34−7.48 (m, 13H, ArH), 8.07−8.36 (m, 9H, PyH); ^{13}C NMR ($CDCl_3$) δ 48.6 (−CH_2NH−), 69.0 (−OCH_2Py), 70.1, 70.2 (−OCH_2Ar), 100.9, 101.7, 101.9, 106.5, 106.6, 106.7, 113.0, 117.8, 123.2, 124.8, 125.1, 125.5, 126.2, 127.0, 127.5, 127.7, 127.8, 128.1, 128.2, 128.7, 129.4, 129.7, 130.9, 131.4, 131.7, 136.9 (Py C), 139.4, 139.5, 142.3 (Ar C), 148.2 (−NHPh C), 160.2, 160.3, 160.4 (−OPh C); MS (MALDI-TOF) *m*/*z* 942.4 (M − 1), 966.4 (M + Na^+), 982.4 (M + K^+), calcd *m*/*z* 943.39.

Py−G3−NHPh. It was prepared from Py−G3−Br and aniline, purified by column chromatography on silica gel (CH_2Cl_2−Et_2O = 300:1) to give Py−G3−NHPh as a pale-yellow glassy solid. Yield 78%; retention time t_R = 21.4 min in HPLC (acetonitrile−THF = 6.5:1), purity 97%; IR ν 3420, 3088, 3062, 3031, 2929, 2871, 1596, 1450, 1375, 1155, 1045 cm^{-1}; ^{1}H NMR ($CDCl_3$) δ

4.26 (s, 2H, $-CH_2N-$), 4.82−5.10 (m, 26H, $-OCH_2Ar$), 5.75 (s, 2H, $-OCH_2Py$), 6.49−6.91 (m, 26H, ArH), 7.20−7.24 (m, 2H, ArH), 7.34−7.46 (m, 33H, ArH), 8.04−8.36 (m, 9H, PyH); ^{13}C NMR ($CDCl_3$) δ 48.5 ($-CH_2NH-$), 69.0 ($-OCH_2Py$), 70.1, 70.2 ($-OCH_2Ar$), 100.9, 101.7, 101.9, 106.5, 106.7, 113.0, 117.7, 123.1, 124.8, 125.0, 125.5, 126.1, 127.0, 127.5, 127.7, 128.1, 128.7, 129.3, 129.7, 130.8, 131.3, 131.7, 136.9 (Py C), 139.4, 142.3 (Ar C), 148.2 (−NHPh C), 160.2, 160.3, 160.4 (−OPh C); MS (MALDI-TOF) *m*/*z* 1790.4 (M − 1), 1814.5 (M + Na^+), 1830.4 (M + K^+), calcd *m*/*z* 1791.72.

Py−G4−NHPh. It was prepared from Py−G4−Br and aniline, purified by column chromatography on silica gel (CH_2Cl_2−Et_2O = 100:1) to give Py−G4−NHPh as a pale-yellow glassy solid. Yield 60%; retention time t_R = 8.4 min in HPLC (acetonitrile−THF = 2:1), purity 97%; IR ν 3420, 3088, 3062, 3030, 2927, 2875, 1594, 1449, 1372, 1152, 1045 cm^{-1}; ^1H NMR ($CDCl_3$) δ 4.13 (s, 2H, $-CH_2N-$), 4.86−4.95 (m, 58H, $-OCH_2Ar$), 5.65 (s, 2H, $-OCH_2Py$), 6.46−6.68 (m, 50H, ArH), 7.06−7.10 (m, 2H, ArH), 7.28−7.35 (m, 73H, ArH), 7.96−8.21 (m, 9H, PyH); ^{13}C NMR ($CDCl_3$) δ 48.4 ($-CH_2NH-$), 69.0 ($-OCH_2Py$), 70.1, 70.2 ($-OCH_2Ar$), 100.8, 101.7, 106.5, 113.0, 117.7, 123.2, 124.8, 125.5, 126.1, 127.0, 127.7, 128.1, 128.7, 129.3, 129.7, 130.9, 131.3, 131.7, 136.9 (Py C), 139.3, 139.5, 142.3 (Ar C), 148.2 (−NHPh C), 160.2, 160.3 (−OPh C); MS (MALDI-TOF) *m*/*z*, 3510.3 (M + Na^+), 3526.2 (M + K^+), calcd *m*/*z* 3488.39.

Acknowledgment. Financial support for this work by National Science Foundation of China (Grant Numbers 20574086, 20603042, and 20733007) and the National Basic Research Program (Grant Number 2007CB808004).

Supporting Information Available: ^1H NMR spectra and HPLC trace figures of Py−G*n*−NHPh and Py−G*n*−OH, fluorescence spectra of Py−G*n*−NHPh and Py−G*n*−OH in CH_2Cl_2, and fluorescence decay curves of Py−G*n*−NHPh and Py−G*n*−OH in CH_2Cl_2. This material is available free of charge via the Internet at http://pubs.acs.org.

References and Notes

(1) Fréchet, J. M. J.; Hawker, C. J. *Comprehensive Polymer Science*, 2nd suppl., ed.; Aggarval, S. L., Russo, S., Eds.; Pergamon: Oxford, U.K., 1996; pp 71−132.
(2) Moore, J. S. *Acc. Chem. Res.* **1997**, *30*, 402.
(3) Tomalia, D. A.; Dvornic, P. R. *Nature* **1994**, *372*, 617.
(4) (a) Philip, D.; Stoddart, J. F. *Angew. Chem., Int. Ed. Engl.* **1996**, *35*, 1154. (b) Watanabe, S.; Regen, S. *J. Am. Chem. Soc.* **1994**, *116*, 8855.
(5) Peppas, N. A.; Nagai, T.; Miyajima, M. *Pharm. Techn. Jpn.* **1994**, *10*, 611.
(6) de Gennes, P. G.; Hervet, H. *J. Phys., Lett.* **1983**, *44*, L351.
(7) Lescanec, R. L.; Muthukumar, M. *Macromolecules* **1990**, *23*, 2280.
(8) Naylor, A. M.; Goddard, W. A., III.; Kiefer, G. E.; Tomalia, D. A. *J. Am. Chem. Soc.* **1989**, *111*, 2339.
(9) Scherrenberg, R.; Coussens, B.; van Vliet, P.; Edouard, G.; Brackman, J.; de Brabander, E.; Mortensen, K. *Macromolecules* **1998**, *31*, 456.
(10) Zhou, T.; Bor, C. S. *Macromolecules* **2005**, *38*, 8554.
(11) Welch, P.; Muthukumar, M. *Macromolecules* **1998**, *31*, 5892.
(12) Mourey, T. H.; Turner, S. R.; Rubinstein, M.; Fréchet, J. M. J.; Hawker, C. J.; Wooley, K. L. *Macromolecules* **1992**, *25*, 2401.
(13) Wooley, K. L.; Klug, C. A.; Tasaki, K.; Schaefer, J. *J. Am. Chem. Soc.* **1997**, *119*, 53.
(14) Gorman, C. B.; Hager, M. W.; Parkhurst, B. L.; Smith, J. C. *Macromolecules* **1998**, *31*, 815.
(15) Hawker, C. J.; Wooley, K. L.; Fréchet, J. M. J. *J. Am. Chem. Soc.* **1993**, *115*, 4375.
(16) De Backer, S.; Prinzie, Y.; Verheijen, W.; Smet, M.; Desmedt, K.; Dehaen, W.; De Schryver, F. C. *J. Phys. Chem. A* **1998**, *102*, 5451.
(17) (a) Chen, J.; Li, S.; Zhang, L.; Liu, B.; Han, Y.; Yang, G.; Li, Y. *J. Am. Chem. Soc.* **2005**, *127*, 2165. (b) Chen, J.; Chen, J.; Li, S.; Zhang, L.; Yang, G.; Li, Y. *J. Phys. Chem. B* **2006**, *110*, 4663. (c) Chen, J.; Li, S.; Zhang, L.; Li, Y. Y.; Chen J.; Yang, G.; Li, Y. *J. Phys. Chem. B* **2006**, *110*, 4047. (d) Zhang, L.; Chen, J.; Li, S.; Chen J.; Li, Y. Y.; Yang, G.; Li, Y. *J. Photochem. Photobiol. A* **2006**, *181*, 429. (e) Chen, J.; Zhang, L.; Li, S.; Li, Y. Y.; Chen Jie.; Yang, G.; Li, Y. *J. Photochem. Photobiol., A* **2007**, *185*, 67.
(18) (a) Taniguchi, Y.; Nishina, Y.; Mataga, N. *Bull. Chem. Soc. Jpn.* **1972**, *45*, 764. (b) Weller, A.; Staerk, H.; Treichel, R. *Faraday Discuss. Chem. Soc.* **1984**, *78*, 271.
(19) (a) Hawker, C. J.; Fréchet, J. M. J. *J. Am. Chem. Soc.* **1990**, *112*, 7638. (b) Hawker, C. J.; Fréchet, J. M. J. *J. Chem. Soc., Chem. Commun.* **1990**, 1010. (c) Hawker, C. J.; Fréchet, J. M. J. *Macromolecules* **1990**, *23*, 4726. (d) Wooley, K. L.; Hawker, C. J.; Fréchet, J. M. J. *J. Chem. Soc., Perkin Trans. 1* **1991**, 1059.
(20) Oevering, H.; Paddon-Row, M. N.; Heppener, M.; Oliver, A. M.; Cotsaris, E.; Verhoeven, J. W.; Hush, N. S. *J. Am. Chem. Soc.* **1987**, *109*, 3258.
(21) (a) Kavarnos, G. J.; Turro, N. J. *Chem. Rev.* **1986**, *86*, 401. (b) Loutfy, R. O. *Photogr. Sci. Eng.* **1976**, *20*, 165.
(22) Dean, J. A. *Lange's Handbook of Chemistry*, 15th ed.; 1998.
(23) (a) Bixon, M.; Jortner, J. *J. Phys. Chem.* **1993**, *97*, 13061. (b) Scully, A. D.; Takeda, T.; Okamoto, M.; Hirayama, S. *Chem. Phys. Lett.* **1994**, *228*, 32. (c) Kroon, J.; Verhoeven, J. W.; Paddon-Row, M. N.; Oliver, A. M. *Angew. Chem., Int. Ed. Engl.* **1991**, *30*, 1358. (d) Inai, Y.; Sisido, M.; Imanishi, Y. *J. Phys. Chem.* **1990**, *94*, 6237. (e) Kwan, P. H.; Swager, T. M. *J. Am. Chem. Soc.* **2005**, *127*, 5902.
(24) (a) Ulstrup, J.; Jortner, J. *J. Chem. Phys.* **1975**, *63*, 4358. (b) Efrima, S.; Bixon, M. *J. Chem. Phys.* **1976**, *64*, 3639. (c) Blumenfeld, L. A.; Chernavskii, D. S. *J. Theor. Biol.* **1973**, *39*, 1.
(25) (a) Brockelhurst, B. *Chem. Phys.* **1973**, *2*, 6. (b) Brockelhurst, B. *J. Phys. Chem.* **1979**, *83*, 536.
(26) Beitz, J. V.; Miller, J. R. *J. Chem. Phys.* **1979**, *71*, 4579.
(27) (a) Capitosti, G. J.; Cramer, S. J.; Rajesh, C. S.; Modarelli, D. A. *Org. Lett.* **2001**, *3*, 1645. (b) Rajesh, C. S.; Capitosti, G. J.; Cramer, S. J.; Modarelli, D. A. *J. Phys. Chem. B* **2001**, *105*, 10175.
(28) (a) Aalbersberg, W. I.; Hoytink, G. J.; Mackor, E. I.; Weijland, W. P. *Mol. Phys.* **1959**, *2*, 3049. (b) Jagur-Grodzinski, J.; Feld, M.; Yang, S. L.; Szwarc, M. *J. Phys. Chem.* **1965**, *69*, 628.
(29) (a) Okada, T.; Karaki, I.; Matsuzawa, E.; Mataga, N.; Sakata, Y.; Misumi, S. *J. Phys. Chem.* **1981**, *85*, 3957. (b) Sato, C.; Kikuchi, K. *J. Phys. Chem.* **1992**, *96*, 5601. (c) Zhang, G.; Thomas, J. K.; Eremenko, A.; Kikteva, T.; Wilkinson, F. *J. Phys. Chem. B* **1997**, *101*, 8569.

MA071901W